Journal of Applied Fluid Mechanics, Vol. 15, No. 5, pp. 1503-1511, 2022.
Available online at www.jafmonline.net, ISSN 1735-3572, EISSN 1735-3645.
https://doi.org/10.47176/jafm.15.05.1168

Numerical Study of the *L/D* Ratio and Turbulent Prandtl Number Effect on Energy Separation in a Counter-Flow Vortex Tube

J. Burazer[1†], Đ. Novković[1], A. Ćoćić[1], M. Bukurov[2] and M. Lečić[1]

[1] *University of Belgrade, Faculty of Mechanical Engineering, Kraljice Marije 16, 11120 Belgrade 35, Serbia*
[2] *University of Novi Sad, Faculty of Technical Sciences, Trg Dositeja Obradovića 6, 21102 Novi Sad, Serbia*

†*Corresponding Author Email: jburazer@mas.bg.ac.rs*

(Received March 11, 2022; accepted May 30, 2022)

ABSTRACT

Vortex tube is a device without moving parts with ability to separate pressurized gas into two streams: cold and hot. This is a consequence of the Eckert-Wiese effect, which is responsible for spontaneous redistribution of total energy within the flow domain. In order for vortex tubes to work properly, there are some constraints which have to be fulfilled. The most important constraint in that sense is the *L/D* ratio. One part of this paper is dedicated to the research of the influence of *L/D* ratio on the energy separation in a vortex tube, i.e. to the values of total temperatures on cold and hot outlets of the device. On the other hand, experimental research of the inner flow is quite challenging since vortex tube is a device of small dimensions. Hence, we are relaying on numerical computations. One of important quantities that has to be prescribed in these computations is the turbulent Prandtl number Pr_T. Because of that, the other part of this paper is dedicated to research of the influence of Pr_T on the results of numerical computations. The research is conducted using open-source software OpenFOAM. Turbulence is modelled using two-equation and RST models. For small *L/D* ratios there is a secondary circulation that acts as a refrigeration cycle, and for greater *L/D* ratios distribution of velocity and temperature inside the vortex tube remains the same, regardless of the stagnation point presence. It is not justified to increase the length of the vortex tube beyond 20*D* since the change in cold total temperature inside the vortex tube as well at the cold outlet is practically null. For *L/D* variation from 1.8 to 10, the cold outlet temperature changes from 270.9 K to 266.8 K, and then rises to its final value of 270.5 K. For *L/D* ratio from 20 to 60, the total temperature at cold end remains unchanged at 271.3 K. We obtained good results with the unit value of turbulent Prandtl number, and demonstrated that increasing the Pr_T beyond unit value is not necessary in order to numerically obtain the energy separation inside the vortex tube.

Keywords: Eckert-Wiese effect; Stagnation point; Parametric optimization; CFD; OpenFOAM.

NOMENCLATURE

D	diameter of the hot tube
D_c	diameter of the cold tube
k	kinetic energy of turbulence
L	length of hot tube
R	radius of the hot tube
R_c	radius of the cold tube
T	static temperature
T_o	total temperature
(x,y,z)	Cartesian coordinates
U	mean velocity in axial (x) direction
ε	dissipation of kinetic energy of turbulence
RSTM	Reynolds Stress Turbulence Model
LG	Launder-Gibson
SST	Shear Stress Transport

Subscripts

T	turbulent
c	cold
h	hot

1. INTRODUCTION

Energy separation, as a consequence of the Eckert-Wiese effect, is a flow-thermodynamic phenomenon that involves spontaneous redistribution of total energy within a flow field, which results in heating of certain parts of this flow field, and cooling of others. This phenomenon was first observed in the 1930s in a vortex tube, and it was later confirmed in the vortex street behind the cylinder, in shear layers, jets.

Despite the fact that the mechanism that provides the stratification of the temperature field in vortex tube is still in some way a mystery, this is a device that can achieve fairly low gas temperatures at the cold outlet. Vortex tube, as a device without moving parts, in which there is a spontaneous stratification of the temperature field, has found application in various areas in everyday life and work. This primarily refers to the machine industry - metal machining and/or sharpening of machine tools, personal cooling of workers exposed to high temperatures at work, instrument cooling, instrument process cooling, etc. Despite low efficiency, prevailing reasons for usage of vortex tube in these applications are compactness, reliability and low equipment cost.

There are several parameters regarding vortex tube's geometry and its working fluid that provide the stratification of the total temperature field in vortex tubes. In order for the vortex tube to work properly, i.e. in order to achieve sufficiently low temperature of the cooled gas at its outlet, it is necessary that certain geometrical relations of the characteristic elements of the vortex tube are satisfied. The important parameters are: L/D ratio, nozzle and hot tube diameters ratio, diameter of the cooled gas outlet, number of nozzles through which the gas is injected into the device. Thermophysical properties of the gas used as a vortex tube working fluid are important as well. In the review paper, Yilmaz *et al.* (2009) characterized important geometric parameters of the vortex tube and thermophysical parameters of the working fluid upon which the vortex tube performance depends. Saidi and Valipour (2003) experimentally tested the influence of thermo-physical and geometrical parameters on energy separation in a vortex tube. The experiments were conducted by varying the inlet pressure and the cold air mass ratio. They determined the optimal value of L/D ratio to be $20 \leq L/D \leq 55.5$, when working fluid is helium and ratio of cold orifice diameter to vortex tube diameter is $d/D = 0.5$ and with three nozzles on the vortex tube. They have determined also that nozzle with more number of flow intakes is causing the decrease in cold air temperature and efficiency. Singh *et al.* (2004) carried out experimental research based upon two designs: maximum temperature drop and maximum cooling effect. They concluded that nozzle design is more important than orifice design for getting higher temperature drops. Also, the length of the vortex tube has no effect on the efficiency of this device when it is increased from 45*D* to 55*D*. Dincer *et al.* (2008) experimentally tested the effects of L/D ratio and number of inlet nozzles on vortex tube performance. They varied the inlet pressure and number of inlet nozzles. These authors concluded that the instability of the stagnation point in the vortex tube occurs for the $L/D = 18$ ratio. A larger temperature drop is achieved at a higher L/D ratio. Behera *et al.* (2005) conducted numerical research in order to optimize the geometry of the vortex tube. They postulated that the increase in the vortex tube's length leads to temperature separation process enhancement up to the condition that the stagnation point is within the length of the vortex tube, which corresponds to the $L/D = 20$ - 30.

All listed applications of vortex tube are localized in a small space. For that reason, it is important that the vortex tube is of acceptable dimensions. The aim of this paper is to establish the connection between flow/temperature fields inside vortex tube and L/D ratio, as a global parameter. Having in mind that the length to diameter ratio is an important parameter for vortex tube's proper functioning, in this paper we will examine if increasing the length of the vortex tube in relation to its diameter, in order to achieve certain temperature at vortex tube cold outlet, is justified. In other words, it will be considered whether it is justified to make a vortex tube of extreme length only to maintain a maximum value of a temperature drop. This paper will present the flow and temperature fields inside the vortex tube for $L/D < 5$, for the first time in literature, to the best of our knowledge.

We will also test the possibility of decreasing the L/D ratio below the value of 5 (for the vortex tube in Bruun (1969) $L/D = 5.5$), in order to determine how this influences the temperature and velocity fields inside vortex tube, and the value of cold outlet total temperature. Hence, we want to see if it is possible to obtain a device of smaller dimensions that produces air of sufficiently low total temperature on the outlet. Also, in numerical calculations value of turbulent Prandtl number is very important. Fröhlingsdorf and Unger (1999) increased its value in order to obtain good agreement between their numerical calculations and experimental results from Bruun (1969). In present research we will examine if this increase of the turbulent Prandtl number is necessary, since it is known that Prandtl number affects the characteristics of heated structure, Kumar and Lal (2021), Tanweer *et al.* (2019). Hence, this parameter is another quantity whose influence on the vortex tube performance will be tested. All computations will be conducted for one working fluid.

2. NUMERICAL COMPUTATIONS

Due to small dimensions of vortex tube, experimental results are scarce. The starting point for our investigation was the vortex tube from Bruun (1969) and Fröhlingsdorf and Unger (1999) which was used for all further computations. Bruun (1969) performed experimental measurements, while Fröhlingsdorf and Unger (1999) used these experimental results for validation of their own numerical findings. Therefore, we have used the results from aforementioned references for validation of our results. We have used both of these investigations to verify our numerical results. The vortex tube in question has hot tube diameter of $D = 2R = 94$ mm, while the length of the hot tube is $L = 520$ mm. The length of the cold tube is L_c=130 mm, while its diameter is $D_c = 2R_c = 35$ mm. Inlet, cold and hot outlets have the same diameter, $d = 16.25$ mm. Geometry of the vortex tube is presented in Fig. 1. Since the gas is injected tangentially through four nozzles that are placed circumferentially in respect to the tube, swirling flow is formed, Bruun (1969). Due to number and arrangement of the nozzles, it can be assumed that flow generated in vortex tube is axisymmetrical. In order to shorten the calculations, we have conducted our computations on a wedge geometry, described in Greenshields (2015).

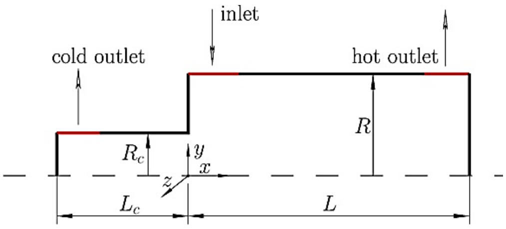

Fig. 1. Computational domain.

All computations in this paper are performed using OpenFOAM - an open-source software, which is basically a set of C++ libraries used in continuum mechanics for numerical computations. With its text-based interface, it is commonly used in scientific research of various kind. For computations in this paper, a steady-state solver steadyCompressibleTEFoam and transient solver rhoCentralTurbFoam are used. These solvers can calculate compressible turbulent flow, and are obtained by modifying existing solvers within OpenFOAM software, which is described in more detail in Burazer (2017). Eckert-Wiese phenomena is already investigated by the OpenFOAM software in flow across cylinder in Burazer (2017, June, 2018), and research on vortex tube's energy separation using modified solvers is presented in Burazer (2017,) and Burazer *et al.* 2019).

For turbulence modeling we have used two of the two-equation models i.e. k-ε and k-ω SST, and Reynolds stress turbulence model - LG (Launder-Gibson). Details on these models can be found in Launder and Sharma (1974) and Menter and Esch (2001, November).

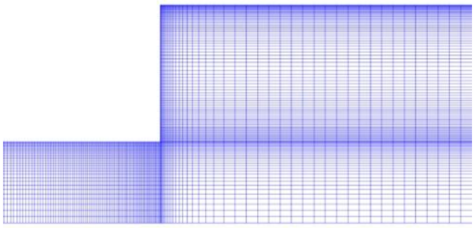

Fig. 2. Detail of one of generated meshes.

Block structured mesh is generated using blockMesh generator from OpenFOAM. In regions of the computational domain where we expect great changes in values of physical quantities, mesh is subjected to fine grading to facilitate the capturing of these changes. Hence, we have to be careful in determination of the dimensionless distance from the wall. Appropriate distances expressed through y+ coordinate are evaluated after the computations are terminated, and meshes are modified accordingly.

We have set the boundary conditions as described in Burazer *et al*. (2019); inlet: fixed temperature and velocity, pressure gradient equal to zero, turbulence intensity 5%; outlet: fixed pressure, inletOutlet boundary conditions for velocity, temperature and turbulence quantities; walls: a no slip boundary condition for velocity and gradient equal to zero of all other quantities. InletOutlet boundary condition allows the possibility of reverse flow on this boundary. When there is no reverse flow, inletOulet boundary condition becomes zeroGradient. For computations in steadyCompressibleTEFoam solver, a fixed value of total enthalpy is set on the inlet, as well.

Discretization of all equation terms, except for turbulence quantities, is carried out by the use of schemes of second order. First order schemes were used for turbulence quantities. In rhoCentralTurbFoam, the convergence criteria is set to 10^{-10} for all physical quantities, except for velocity which is set to 10^{-9}, while for steadyCompressibleTEFoam, tolerances for all physical quantities are set to 10^{-8}. The prescribed relative tolerance for all quantities in both solvers is set to zero. Maximum value of Courant number $Co_{max} = 0.3$ is used for the control of time step size in transient solver.

The working fluid is air, that is regarded as calorically perfect gas ($Pr = 0.7$, $c_p = 1004.5$ J/(kgK)).

3. Results and Discussion

3.1 Influence of mesh size to test results

The mesh independence analysis is performed. Results of this mesh independence study are already presented in Burazer *et al*. (2017). It is important to state that calculations are performed on three different mesh sizes with 26500 (M1), 31500 (M2) and 36040 (M3) cells. Based on total temperature distributions presented in Fig. 3, it is evident that mesh M2 is selected for all computations regarding this vortex tube. Similar distributions of total temperature are obtained with transient solver. Hence, results for mesh M2 are presented in this paper.

As we have demonstrated in Burazer *et al*. (2017), solver rhoCentralTurbFoam in combination with k-ε model gives the best results when predicting the outlet temperatures. Computations with transient solver rhoCentralTurbFoam take too long, since the average value of the time step is of the order of 10^{-8},

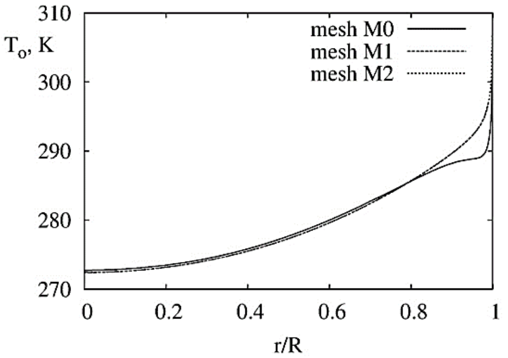

Fig. 3. Mesh independence study results, cross section *x*/*L* = 0.23, solver, *k*-*ε* model, steady Compressible TEFoam.

Burazer *et al*. (2017). In order to shorten the computational time, we have selected to do the computations for Pr_T and *L*/*D* variations using *k*-*ε* model in combination with a steady-state solver – steadyCompressibleTEFoam, whose results are within the margin of 1% from the experimentally obtained values, Burazer *et al*. (2017).

3.2 Influence of turbulent Prandtl number on energy separation

Turbulent Prandtl number Pr_T is a dimensionless parameter that represents the ratio of turbulent viscosity ν_T and turbulent thermal diffusivity α_T, i. e.

$$Pr_T = \nu_T / \alpha_T .$$

The simplest model for turbulent Prandtl number prediction is the Reynolds analogy, which yields that $Pr_T = 1$. This value is correct for most number of boundary layer flows, and it is adopted in this paper's research, as a preset value in all OpenFOAM software solvers. Nevertheless, we have also performed computations with different values of Pr_T. Fröhlingsdorf and Unger (1999) have already performed this type of calculations. They have increased the value of Pr_T in order to achieve the energy separation in vortex tube and good agreement with experimental results from Bruun (1969). Results of our calculations are presented in Fig 4.

Figure 4 shows the influence of the value of turbulent Prandtl number Pr_T on distributions of static temperature *T* and stagnation temperature T_o on hot and cold outlets of vortex tube. This figure confirms that the turbulent Prandtl number really has an influence on temperature values on vortex tube's outlets. As expected, this influence is greater in the field of heated gas temperatures, both static and stagnation. It can be seen that with turbulent Prandtl number increase, both static and total cold outlet temperature almost linearly increase. On the other hand, static temperature of hot air decreases with Pr_T increase, while total temperature first decreases and then increases, with minimum range of values. Obviously, total temperature at cold and hot outlet of the vortex tube has higher values than corresponding static temperature. One of the

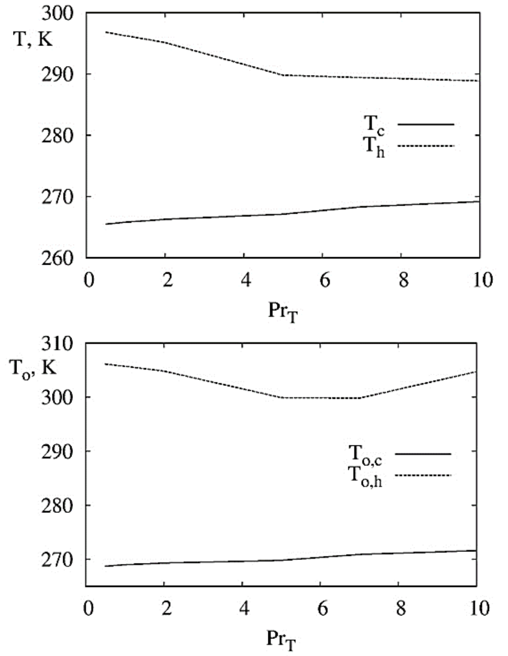

Fig. 4. Influence of turbulent Prandtl number Pr_T on average value of static temperature *T* and stagnation temperature T_o on vortex tube's cold and hot outlets.

guidelines in designing vortex tubes is to obtain maximal energy separation, Eiamsa-ard and Promvonge (2008). In that sense, it is important to examine the influence of turbulent Prandtl number Pr_T on the energy separation intensity, represented with the difference in total temperatures on hot and cold outlets of a vortex tube. It is obvious that with Pr_T increase the temperature difference at the outlets of the vortex tube decreases, as shown in Fig. 4. The main reason for this is the monotonous rise of the cold outlet temperature, but there is also the change in hot outlet temperature, which is more influenced by the turbulent Prandtl number, as it was mentioned before.

If we limit to the extreme values of the turbulent Prandtl number that are considered in the research, it can be concluded that maximum energy separation is achieved for minimal value of turbulent Prandtl number, i.e. for $Pr_T = 0.5$. In that case, cold outlet temperature is at its minimum, and the hot outlet temperature has its maximum value. These findings are in disagreement with the research Fröhlingsdorf and Unger (1999). Fröhlingsdorf and Unger (1999) varied the value of turbulent Prandtl number and the change of averaged values of total temperatures at the outlets of the vortex tube was observed. These values are shown in Table 1. As one can see, with the increase in Pr_T, the value of cold outlet total temperature decreases, until it reaches the value close to experimentally obtained in Bruun (1969). This cold outlet total temperature value is obtained for Pr_T = 9. Together with the results from Fröhlingsdorf and Unger (1999), the results of the calculations carried out within the research in this paper are also presented. The average values of the total temperature obtained by applying three different turbulence models are given, all for the same, unit value of the turbulent Prandtl number, i.e. $Pr_T = 1.0$. As stated earlier, the unit value of the turbulent Prandtl number is a preset value in OpenFOAM software and we decided to adopt it since the working fluid in vortex tube is air. For this value of turbulent Prandtl number, using *k*-*ω* SST turbulence model and rhoCentralTurbFoam solver, we obtained practically the same results for total temperature as the authors of Fröhlingsdorf and Unger (1999) did for $Pr_T = 9$. This outcome, i.e. the best agreement with experimental values of total temperature for turbulent Prandtl number $Pr_T = 1.0$ is in accordance with previously presented research, both experimental and numerical, from the aspect of the value of the turbulent Prandtl number that is adopted in calculations. Depending on the laminar Prandtl number value, the turbulent Prandtl number should be defined in the range of 0.7 to 0.9. Higher value of turbulent Prandtl number is justified when the heat transfer of fluids with higher values of thermal conductivity is considered, Kays (1994). This is for example, the case of liquid metals, Vodret *et al.* (2014). In listed paper the authors suggested changes in the way turbulent Prandtl number is determined with intention of making this a higher value. Our results with aforementioned OpenFOAM solvers show that increasing the turbulent Prandtl number is not justified and leads to violation of physics of the considered problem.

Table 1. Present numerical results in comparison with experimental values from Bruun (1969) and numerical results Fröhlingsdorf and Unger (1999).

Vortex tube entry: T_o=294 K	$T_{o,c}$, K	$T_{o,h}$, K	Pr_T
Experiment, Bruun (1969)	273.9	299.9	-
CFX, Fröhlingsdorf and Unger (1999)	283.4	297.2	0.9
	280.2	298.2	1.8
	278.2	298.9	2.7
	273.9	300.2	9.0
rhoCentralTurbFoam, *k*-*ε*	273.8	301.1	1.0
rhoCentralTurbFoam, SST	274.2	300.3	1.0
rhoCentralTurbFoam, LG	276.4	300.8	1.0
steadyCompressibleTEFoam, *k*-*ε*	275.9	303.5	1.0

From Table 1 it can be seen that transient solver rhoCentralTurbFoam with *k*-*ε* and *k*-*ω* SST models has the best results compared with the experimental values from Bruun (1969), for cold and hot outlet total temperature, respectively. The RSTM gives slightly higher values of the temperature on cold outlet, and approximately the same value of the hot outlet total temperature. Also, steady-state solver steadyCompressibleTEFoam has results that are close to the experimental values. So, we have demonstrated that independently of the solver and the turbulence model, there is no need in altering the value of the turbulent Prandtl number in order to obtain better results. Therefore, there is no physical justification in increasing Pr_T for a single fluid in order to obtain better numerical results, since this violates the physics of the flow.

Certainly, additional research is necessary, since there is a deviation in hot total temperature distribution with the change in turbulent Prandtl number values.

3.3 Influence of *L*/*D* ratio on energy separation

This ratio is considered to be one of the most important parameters for the operation of the vortex tube. Previous experimental and numerical studies presented in Saidi and Valipour (2003) and Singh *et al.* (2004) have shown that increasing the length of the vortex tube has a positive effect on the stratification of the total temperature field in the vortex tube, but also that there is an optimal value of *L*/*D* ratio. Its further increase has no effect on the intensity of the energy separation in the vortex tube. This optimal value is *L*/*D* = 45 according to Yilmaz *et al*. (2009). It is suggested in Behera *et al*. (2005) that increasing the length of the vortex tube has a positive effect on the intensity of stratification of the total temperature field, as long as the stagnation point is inside the vortex tube. In this research we have changed the *L*/*D* ratio by altering the length of vortex tube *L*, with fixed value of diameter *D*.

Figure 5 shows the dependence of the total temperature at the cold and hot outlets with *L*/*D* ratio. Precisely, this figure presents the change of energy separation intensity with the *L*/*D* ratio. According to this, increase of *L*/*D* ratio above 20 has practically insignificant influence on energy separation intensity, as it is shown in Singh *et al.* (2004). It is noticed that the *L*/*D* ratio affects more the total temperature at the outlet with hot gas. At higher values of the considered parameter, the values of total and static temperature of the hot gas are approximately the same. Hence, sufficient increase of the vortex tube length, causes the decrease of the flow rate of heated gas. At the cold end, this is not the case, as expected. There is a deviation in total temperature on cold outlet for small values of *L*/*D* ratio (Fig. 5). The total temperature drops from 270.9 K to 266.8 K, and then rises to its final value of 270.5 K (see Table 2). Explanation of this phenomenon could be as follows.

Figures 6 through 8 present distributions of axial velocity on one half, and total temperature on the other half of the meridian plane of vortex tubes of different lengths, i.e. different *L*/*D* ratios. These figures also present the contours of total temperature with the value of $T_{o,c}$, as well as the zero axial velocity contours. When we compare the values of $T_{o,c}$ with minimum values of total temperature on the corresponding legends, it is obvious that even lower values of total temperatures are obtained inside vortex tubes in comparison to their values on the cold outlets. The lowest value of total temperature on the cold outlet is achieved for *L*/*D* = 2.8, but the lowest temperature inside vortex tube is achieved for *L*/*D* = 1.4. The later may be attributed to secondary circulation inside vortex

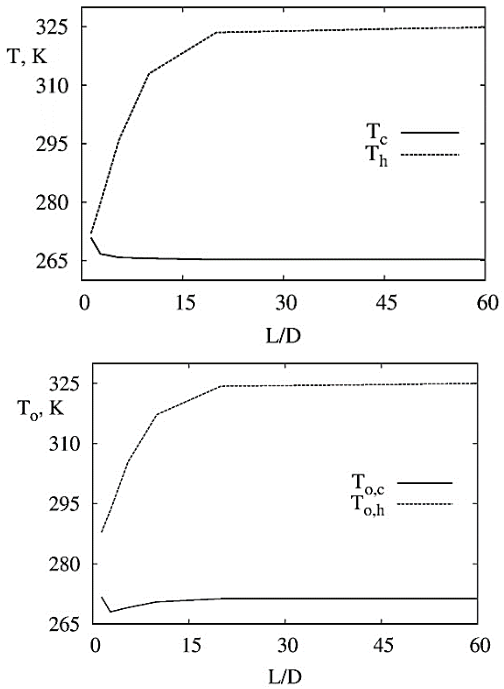

Fig. 5. *L/D* ratio influence on the average value of temperature *T* and total temperature T_o on cold and hot outlets.

tube, which acts as refrigeration cycle inside the device, as shown in Ahlborn and Gordon (2000). However, when this cooler gas reaches the entry of cold tube, in the case of *L*/*D* = 1.4 there is resistance in the form of the gas backflow in the central part of the device. Since the lowest stagnation temperature is achieved in central part of vortex tube, it is clear that the gas with this lowest value of total temperature can't flow towards the cold outlet. In vortex tube of *L*/*D* = 2.8 the backflow is not expressed to that extent. Hence, there is a full cross-sectional flow of cooled gas from hot to cold pipe end. This is the case with all other considered vortex tubes presented in Figs. 7 and 8. It is also evident from Fig. 6, that increase in tube length *L* causes significant increase in the magnitude of axial velocity in the negative side of longitudinal axis. The appearance of this secondary circulation only for *L*/*D* = 1.4 ratio is contrary to the claims of Behera *et al.* (2005). They postulated that secondary circulation happens only with small ratio of cold outlet orifice and vortex tube diameter. In our case, the secondary circulation appearance is in relation to the *L*/*D* ratio of the vortex tube (all other parameters are the same).

Figure 7 presents distribution of total temperature and axial velocity in vortex tubes with *L*/*D* ratio of 10 and 20. There is no stagnation point inside the vortex tube. Considering total temperature legends and the values of total temperatures on cold outlets listed in Table 2 and represented as contours in Fig. 7, we can say that in these vortex tubes lower values of total temperatures are achieved, compared to that on the cold outlet, as well. However, unlike the vortex tubes presented in Fig. 6, in which the minimum value of stagnation temperature is

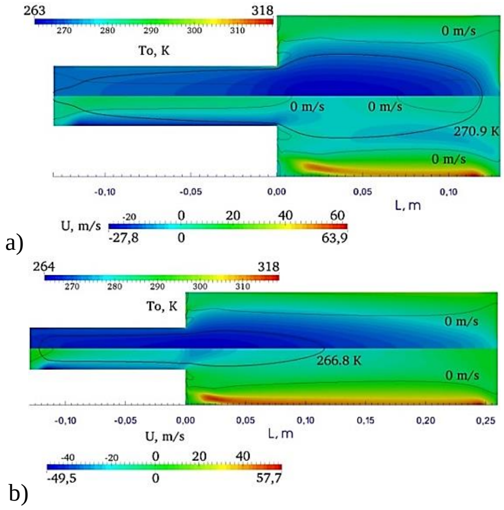

a)

b)

Fig. 6. Axial velocity and total temperature fields in case a) *L*/*D* = 1.4 and b) *L*/*D* = 2.8.

Table 2. Averaged values of total temperature on cold and hot outlets.

L/*D*	$T_{o,h}$, K	$T_{o,c}$, K	Label
1.4	272.1	270.9	L_1
2.8	279.7	266.8	L_2
10	317.2	270.5	L_3
20	324.4	271.3	L_4
50	324.8	271.3	L_5
60	324.9	271.3	L_6

achieved in the central part of the device, here, this minimum value is achieved in a cold tube. It is interesting to note that in vortex tubes from Fig. 7, the stagnation point in cold tube is practically on the wall close to the cold outlet, and that in vortex tubes of smaller *L*/*D* ratio (see Fig. 6), this stagnation point is away from that wall. Also, it is noticeable that with the increase in vortex tube's length, the zone of cold total temperatures, about 280 K and lower, is localized in the first 200 mm of the hot tube length. As we can see in Fig. 6, this cold zone is distributed along the whole length of the hot tube, and the farthest point in the total temperature contour with the value of that on cold outlet, is at about 120 mm of the hot tube length, even though the length of the vortex tube in Fig. 6b is twice the length of the vortex tube presented in Fig. 6a. According to legends of total temperature in Fig. 7, the minimum value of total temperature in both vortex tubes is the same.

In the case of vortex tubes presented in Fig. 6, the axial velocity in the negative direction of *x*-axis for vortex tube with *L*/*D* = 2.8 has almost twice the value of the same velocity in vortex tube *L*/*D* = 1.4. This is a consequence of the fact that in the case of a shorter vortex tube this velocity is achieved in a near-wall region of a cold tube, due to presence of a flow in positive *x*-direction of coaxial part. In Fig. 6b can be seen that this velocity is achieved in the coaxial part of the cold tube. In the case of vortex tubes presented in Fig. 7, this is not the case. Even

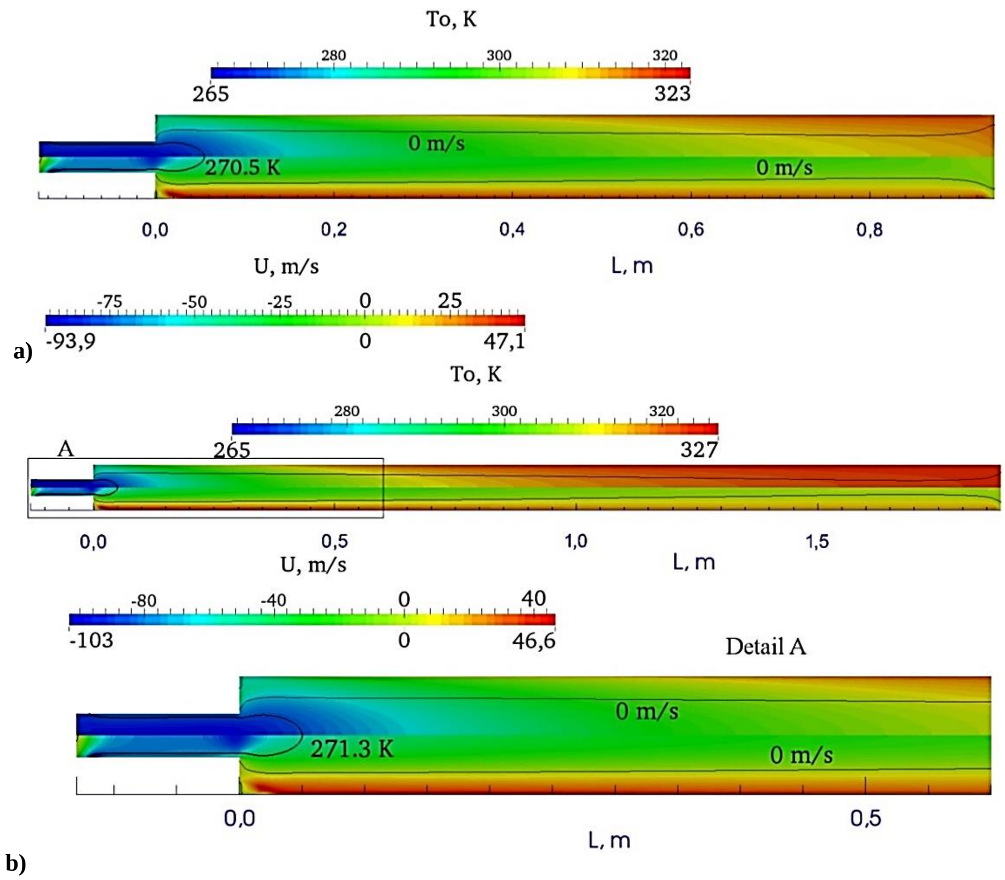

Fig. 7. Axial velocity and total temperature fields in cases for a) *L*/*D* = 10, b) *L*/*D* = 20.

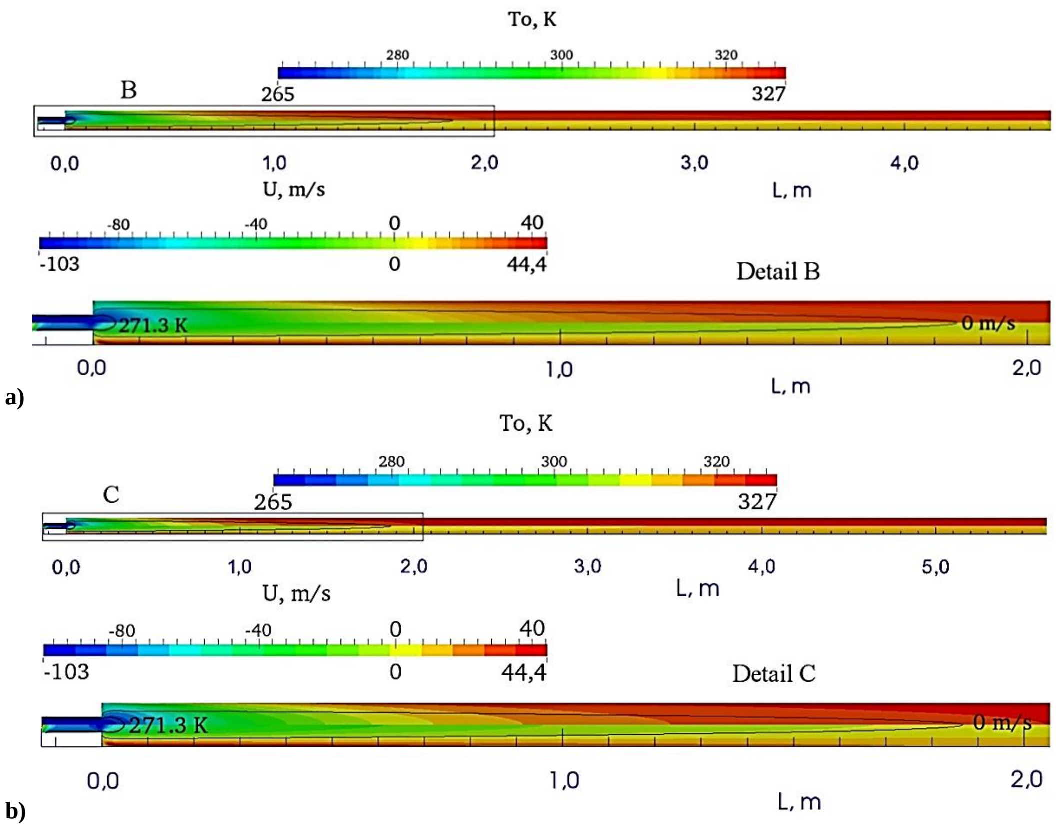

Fig. 8. Axial velocity and total temperature fields in cases of a) *L*/*D* = 50 and b) *L*/*D* = 60.

though the vortex tube in Fig. 7b is twice the length of that in Fig. 7a, the flow structure inside these vortex tubes is the same; the stagnation point in the cold tube is very close to the wall, close to the cold outlet; and in both cases, the maximum value of negative axial velocity is achieved in a coaxial part of the cold tube's flow. It can be concluded that the mass flow rate of the cold gas is somewhat greater in the case of a vortex tube with greater *L*/*D* ratio.

Vortex tubes presented in Fig. 8 have an *L*/*D* ratio of 50 and 60. Contrary to previous values of *L*/*D* ratios, here we have stagnation points in both vortex tubes. What is characteristic for these two vortex tubes is that the position of stagnation point along the *x*-axis doesn't change much with increase of the *L*/*D* ratio from 50 to 60 (see Details B and C in Fig. 7). The cold outlet total temperature in these vortex tubes is the same as in the case of *L*/*D* = 20. Also, the minimum value of total temperature is the same as in vortex tube presented in Fig. 7b. Both total temperature and axial velocity legends for vortex tubes in Fig. 8 are completely the same, as these two in Fig. 7b. This means that cold gas mass flow rate is the same as in the case of a vortex tube from Fig. 7b.

When we compare the average values of total temperatures presented in Table 2 that correspond to the values in Figs. 6 through 8, we can conclude that the same $T_{o,c}$ is obtained for *L*/*D* from 20 to 60. The lowest $T_{o,c}$ is obtained for *L*/*D* = 2.8 (see Table 2). However, the minimum value of total temperature of cooled gas is achieved inside the vortex tube of *L*/*D* = 1.4 (see Fig. 6a). The later is also show in Fig. 9, where the values of total temperature along the vortex tube axis for different *L*/*D* ratios are presented.

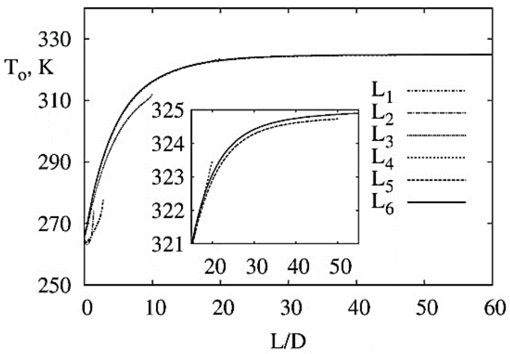

Fig. 9. Total temperature distribution along the axis of vortex tubes of different lengths.

From this Figure it is obvious that, excluding vortex tubes of the lowest *L/D* ratio – L_1 and L_2, the coldest gas along the axis of a vortex tube is achieved in vortex tube with *L*/*D* = 10. Further, increasing the length of vortex tube from 50*D* to 60*D* leads to increase of the total temperature in the tube's axis. The only parameter that increases with *L*/*D* ratio increase from 20 to 60 is the temperature difference obtained on the outlets of the vortex tube, which confirms research conducted in Singh *et al*. (2004), but that increase is not so high, and it is a consequence of a slight increase in hot outlet temperature as shown in Table 2. So, if the length of the vortex tube is three times increased, i.e. from 20*D* to 60*D*, there is no change in cold outlet temperature, with slight increase in hot outlet total temperature resulting in slight increase of energy separation intensity on the vortex tube's outlets.

4. SUMMARY

Numerical research on the Pr_T and *L*/*D* ratio influence on the flow and temperature distributions inside vortex tube is performed in this paper. Turbulent Prandtl number Pr_T is a significant parameter used in determining the heat flux in a vortex tube, while the *L*/*D* ratio is probably the first parameter considered when designing a vortex tube.

Qualitative agreement with previous research regarding the value of the turbulent Prandtl number adopted in the calculations was established. It is shown that for unit value of this quantity we have obtained fairly good agreement with experimental results. It is demonstrated that increasing this quantity in order to obtain appropriate values of total temperature on the vortex tube's outlets is not necessary, nor justified, contrary to research conducted in Fröhlingsdorf and Unger (1999). Additional research is necessary to analyze the flow in near-wall region inside the vortex tube. We have also obtained qualitative agreement with previous research regarding the behavior of the vortex tube with variation of its length at constant diameter. We have presented within this research the velocity and temperature fields inside the vortex tube for different *L*/*D* ratios. It is shown that the lowest value of total temperature inside the vortex tube is obtained for *L*/*D* = 1.4, since there is a secondary circulation inside the device that acts as a refrigeration cycle and can be responsible for lowering the gas temperature. This was also shown in Ahlborn and Gordon (2000). This low value of total temperature is not achieved on the outlet, due to backflow in the cold tube of the device. The lowest value of the total temperature on the cold outlet is obtained for *L*/*D* = 2.8. For *L*/*D* ≥ 10 the distribution of velocity and temperature inside the vortex tube remains the same. Stagnation point appears for *L*/*D* = 50, and remains at the same place when the length of vortex tube is increased from 50*D* to 60*D*. The temperature field as well the value of total temperature on the cold outlet remains the same, regardless of the stagnation point presence in the flow field for *L*/*D* ≥ 20.

Presented results create the possibility of designing a vortex tube in a numerical way, by conducting analysis on how certain parameters influence on the operation of the vortex tube. In this case we could design a vortex tube of optimal geometry for different purposes.

ACKNOWLEDGMENT

This research was funded by the grant from the Ministry of Education, Science and Technological

Development, Republic of Serbia under the Contract No. 451-03-9/2021-14/200105 (subproject TR35046), and by Science Fund of the Republic of Serbia through project "Research and development of ionic biofluids - RIDIBF" which is implemented within the Program for excellent projects of young researchers - PROMIS, which authors hereby gratefully acknowledge.

REFERENCES

Ahlborn, B. K. and J. M. Gordon (2000). The vortex tube as a classic thermodynamic refrigeration cycle, *Journal of Applied Physics* 88(6), 3645-3653,

Behera, U, P. J. Paul, S. Kasthurirengan, R. Karunanithi, S. Ram, K. Dinesh, and S. Jacob (2005). CFD Analysis and Experimental Investigation Towards Optimizing the Parameters of Ranque-Hilsch Vortex Tube, *Int. Journal of Heat and Mass Transfer* 48(10), 1961-1973.

Bruun, H. H. (1969). Experimental Investigation of the Energy Separation in Vortex Tubes, *J. Mechanical Engineering Science* 11(6), 567-582.

Burazer, J. M, A. S. Ćoćić and M. R. Lečić (2017). Numerical research of the compressible flow in a vortex tube using OpenFOAM software, *Thermal Science* 21(Suppl. 3), S745-S758.

Burazer, J. M, Đ. M. Novković, D. M. Knežević and M. R. Lečić (2019). Numerical research of compressible turbulent swirl flow with energy separation in a cylindrical tube, *FME Transactions* 47(1), 16-22.

Burazer, J. M. (2018). Energy separation in transient and steady-state flow across the cylinder, *Theoretical and Applied Mechanics* 45(1), 83-94.

Burazer, J. M. (2017, June). Numerical research of energy separation in a cylinder wake, in *Proceedings of the 6th International Congress of Serbian Society of Mechanics, Turbulence Minisymposium*, Mountain Tara, Serbia, Paper M2i, 8 pages

Burazer, J. M. (2017). *Turbulent compressible flow in a Ranque-Hilsch vortex tube*, Doctoral Dissertation, Faculty of Mechanical Engineering, University of Belgrade, Belgrade, Serbia (in Serbian)

Dincer, K, S. Baskaya and B. Z. Uysal (2008). Experimental investigation of the effect of length to diameter ratio and nozzle number on the performance of counter flow Ranque-Hilsch vortex tube, *Heat Mass Transfer* 44(3), 367-373.

Eiamsa-ard, S. and P. Promvonge (2008). Review of Ranque-Hilsch effects in vortex tubes, *Renewable and Sustainable Energy Reviews* 12(7), 1822-1842.

Fröhlingsdorf, W. and H. Unger (1999). Numerical Investigations of the Compressible Flow and the Energy Separation in the Ranque-Hilsch Vortex Tube, *International Journal of Heat and Mass Transfer* 42(3), 415 - 422.

Greenshields, C. J. (2015). *OpenFOAM, The Open Source CFD Toolbox User Guide*. Version 3.0.1, CFD Direct Ltd.

Kays, W. M. (1994). Turbulent Prandtl number – Where are we? *Transactions of ASME. Journal of Heat Transfer*, 116(2), 284-295.

Kumar, S. A. and S. A. Lal (2021). Effects of Prandtl number on three dimensional coherent structures in the wake behind a heated cylinder, *Journal of Applied Fluid Mechanics*, 14 (2), 515-526.

Launder, B. and B. Sharma (1974). Application of the Energy Dissipation Model of Turbulence to the Calculation of Flows Near a Spinning Disk, *Letters in Heat and Mass Transfer* 1(2), 131-138.

Menter, F. and T. Esch (2001, November). Elements of Industrial Heat Transfer Predictions, *Proceedings of COBEM 2001*, Invited Lecture, Uberlandia, Minas Gerais, Brazil, Vol. 20, 117-127

Saidi, M. H. and M. S. Valipour (2003). Experimental modeling of a vortex tube refrigerator, *Applied Thermal Engineering* 23(15), 1971-1980.

Singh, P. K, R. G. Tathgir, G. Dasaroju and G. S. Grewal (2004). An experimental performance evaluation of vortex tube, *Journal of the Institution of Engineers (India): Mechanical Engineering Division* 84(4), 149-153.

Tanweer, S, A. Dewan and S. Sanghi (2019). Study on effects of Prandtl number on cross buoyancy flow past a square cylinder using OpenFOAM, *Journal of Applied Fluid Mechanics*, 12 (1), 257-269.

Vodret, S, D. Vitale Di Maio and G. Caruso (2014). Numerical simulation of turbulent forced convection in liquid metals, *Journal of Physics: Conference Series* 547 012033.

Yilmaz, M, M. Kaya, S. Karagoz and S. Erdogan (2009). A review on design criteria for vortex tubes, *Heat Mass Transfer* 45(5), 613-632.